Title
The enhanced drying effect of Central-Pacific El Niño on US winter

Journal
Environmental Research Letters, 8(1)

Authors
Yu, Jin-Yi
Zou, Yuhao

Publication Date
2013-03-01

Peer reviewed

The enhanced drying effect of Central-Pacific El Niño on US winter

2013 Environ. Res. Lett. 8 014019

(http://iopscience.iop.org/1748-9326/8/1/014019)

OPEN ACCESS
IOP Publishing ENVIRONMENTAL RESEARCH LETTERS
Environ. Res. Lett. **8** (2013) 014019 (7pp) doi:10.1088/1748-9326/8/1/014019

The enhanced drying effect of Central-Pacific El Niño on US winter

Jin-Yi Yu and Yuhao Zou

Department of Earth System Science, University of California, Irvine, CA 92697-3100, USA

E-mail: jyyu@uci.edu

Received 10 December 2012
Accepted for publication 22 January 2013
Published 12 February 2013
Online at stacks.iop.org/ERL/8/014019

Abstract
In what is arguably one of the most dramatic phenomena possibly associated with climate change or natural climate variability, the location of El Niño has shifted more to the central Pacific in recent decades. In this study, we use statistical analyses, numerical model experiments and case studies to show that the Central-Pacific El Niño enhances the drying effect, but weakens the wetting effect, typically produced by traditional Eastern-Pacific El Niño events on the US winter precipitation. As a result, the emerging Central-Pacific El Niño produces an overall drying effect on the US winter, particularly over the Ohio–Mississippi Valley, Pacific Northwest and Southeast. The enhanced drying effect is related to a more southward displacement of tropospheric jet streams that control the movements of winter storms. The results of this study imply that the emergence of the Central-Pacific El Niño in recent decades may be one factor contributing to the recent prevalence of extended droughts in the US.

Keywords: Central-Pacific El Niño, US winter, precipitation, Eastern-Pacific El Niño, stormtrack, drought

1. Introduction

The climate in the United States (US) is significantly influenced by El Niño events in the tropical Pacific (e.g., Ropelewski and Halpert 1986, 1989, Kiladis and Diaz 1989, Livezey *et al* 1997, Dettinger *et al* 1998, Mo and Higgins 1998, Montroy *et al* 1998, Cayan *et al* 1999, Larkin and Harrison 2005b; and many others). The influences on the winter climate are often described as a seesaw pattern as the northern US tends to be warmer and drier than normal while the southern US tends to be colder and wetter than normal. However, the recent recognition of the existence of different flavors or types of El Niño (Wang and Weisberg 2000, Trenberth and Stepaniak 2001, Larkin and Harrison 2005a, Yu and Kao 2007, Ashok *et al* 2007, Guan and Nigam 2008, Kao and Yu 2009, Kug *et al* 2009) has prompted efforts to refine this classical view and to differentiate the impacts according to the El Niño type. The two specific El Niño types that have recently been emphasized are the Eastern-Pacific (EP) El Niño and the Central-Pacific (CP) El Niño (Yu and Kao 2007, Kao and Yu 2009). EP El Niño events are characterized by sea surface temperature (SST) anomalies extending along the equator westward from the South American Coast, while the CP El Niño events are characterized by SST anomalies mostly confined to a region near the equator around the international dateline. While the EP type used to be the conventional type of El Niño, the CP type has occurred more frequently in the past few decades (Ashok *et al* 2007, Kao and Yu 2009, Kug *et al* 2009, Lee and McPhaden 2010, Yu *et al* 2012a). The shift in the location of the SST anomalies can lead to different atmospheric responses (Kumar and Hoerling 1995, Mo and Higgins 1998, Hoerling and Kumar 2002, Barsugli and Sardeshmukh 2002, DeWeaver and Nigam 2004) to these two types of El Niño and result in different impacts on US climate.

Two recent studies (Mo 2010 and Yu *et al* 2012b), for example, have shown that the El Niño impacts on US winter temperatures are different for the CP and EP types and that the typical warm-north, cold-south impact pattern is a mixture of the different impacts produced by the two types of El Niño. According to the studies, different temperature impacts are produced because different wave trains are excited in the extratropical atmosphere when the El Niño SST anomalies are located near the international dateline (CP type) as opposed to near the South American coast (EP type). The CP El Niño excites a wave train resembling the Pacific/North American (PNA; (Wallace and Gutzler 1981) pattern, while the EP El Niño excites a polarward wave train emanating straight out of the tropics into higher latitudes (see figure 5 of Yu *et al* (2012b)). The different wave train responses should also affect the locations and strengths of tropospheric jet streams that control the winter storm paths over the US. In this study, we conduct statistical analyses of reanalysis data, numerical experiments with a forced atmospheric general circulation model and case studies of the major El Niño events since 1948 to examine the impacts of the two types of El Niño on US winter precipitation.

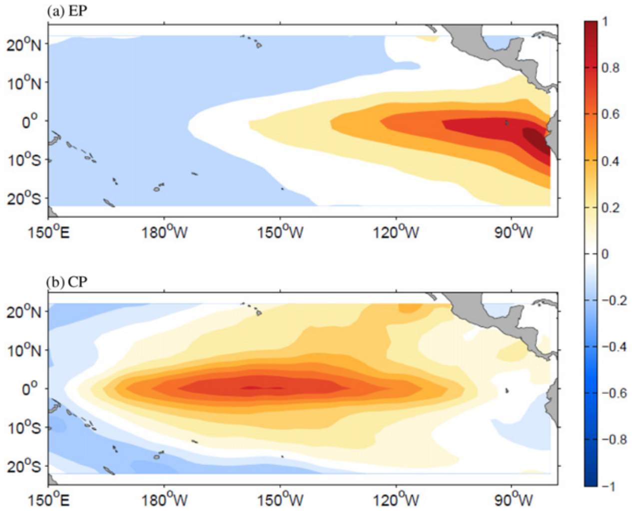

Figure 1. EOF patterns of sea surface temperature anomalies obtained from a regression–EOF method for: (a) the EP type of El Niño and (b) the CP type of El Niño.

2. Data and analysis methods

This study uses two data products for the analyses: SSTs from the National Oceanic and Atmospheric Administration (NOAA)'s Extended Reconstructed Sea Surface Temperature (ERSST) V3b dataset (Smith and Reynolds 2003) and precipitation and wind data from the National Centers for Environmental Prediction–National Center for Atmospheric Research (NCEP–NCAR) Reanalysis (Kistler *et al* 2001). Monthly SST, precipitation and wind anomalies from 1948 to 2010 were analyzed. Anomalies are defined as deviations from the 1948–2010 climatology.

Monthly values of the EP Niño index and the CP El Niño index from Yu *et al* (2012a, 2012b) were used to represent the intensities of the two types of El Niño. The indices were constructed from the monthly SST data using a regression–EOF analysis (Kao and Yu 2009, Yu and Kim 2010). In this method, the SST anomalies regressed with the Niño1+2 (0°–10°S, 80°W–90°W) SST index were removed before the EOF analysis was applied to obtain the spatial pattern of the CP El Niño. The regression with the Niño1+2 index was used as an estimate of the influence of the EP El Niño and was removed to better reveal the SST anomalies associated with the CP El Niño. Similarly, we subtracted the SST anomalies regressed with the Niño4 (5°S-5°N, 160°E-150°W) index (i.e., representing the influence of the CP El Niño) before the EOF analysis was applied to identify the leading structure of the EP El Niño. Figure 1 shows the leading EOF modes obtained from this analysis that exhibit the typical SST anomaly patterns of these two types of El Niño. For the EP El Niño (figure 1(a)), the warm anomalies extend from the South American coast to the central Pacific. As for the CP El Niño (figure 1(b)), the warm anomalies are confined in the tropical central Pacific near the international dateline. The associated principal components from these two leading EOF modes represent the strengths of these two types of El Niño and are defined as the CP El Niño index and the EP El Niño index, respectively.

We also conducted three ensemble forced experiments with an atmospheric general circulation model (AGCM) to contrast the impacts produced by the two types of El Niño. The AGCM used is the Version 4 of the Community Atmosphere Model (CAM4) from the National Center for Atmospheric Research. The three experiments include a control run, an EP run and a CP run. In the control run, climatological, annually cycled SSTs (calculated from 1948–2010) are used as the boundary condition to force CAM4. For the EP (CP) run, the CAM4 is forced by SSTs constructed by adding together the climatological SSTs and SST anomalies associated with the EP (CP) El Niño. The SST anomalies used in the latter two experiments are constructed by regressing tropical Pacific anomalies with the EP and CP El Niño indices and then scaling them to typical El Niño magnitudes. For each of the runs, a 10-member ensemble of 22-month-long integrations was conducted with the El Niño SST anomalies evolving through a developing phase, peak phase, and decaying phase. The peak phases of the SST anomalies were placed in December of Year 1 for each member.

3. Results

We first regressed US winter (January–February–March; JFM) precipitation anomalies to the EP and CP El Niño indices to identify the impact patterns. The regression coefficients with the US winter precipitation are displayed in figures 2(a)–(b), with the hatches indicating the data points where the coefficients pass the student-t test at the 90% significance level. The figures show that both types of El Niño produce a dry-north, wet-south anomaly pattern, similar to the seesaw pattern that has traditionally been used to describe the El Niño impacts on US winter precipitation. The dry and wet anomalies are largely along the eastern and western

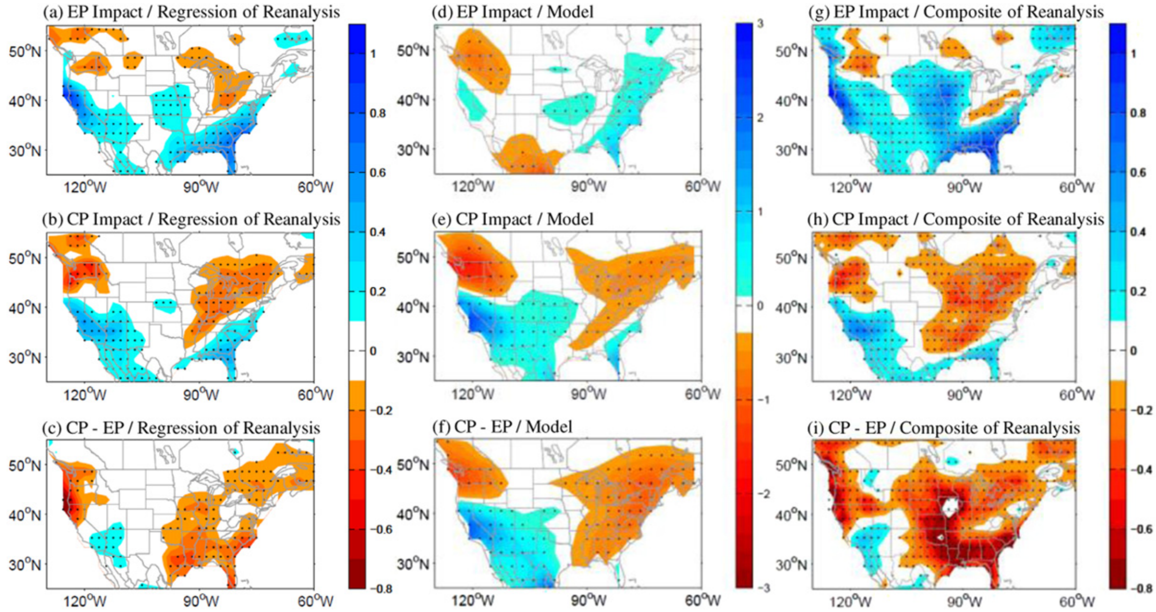

Figure 2. US winter (January–February–March; JFM) precipitation anomalies associated with the El Niño are shown in the top panels for the EP El Niño, in the middle panels for the CP El Niño, and in the bottom panels for the difference between the two types of El Niño (i.e., CP impact minus EP impact). The values shown in the left column (a)–(c) are obtained by regressing US winter precipitation anomalies to the EP and El Niño index. The values shown in the second column (d)–(f) are calculated by subtracting the ensemble-mean winter precipitation of the forced AGCM experiments from the ensemble means of the EP and CP runs. The values shown in the right column (g)–(i) are obtained by compositing major EP and CP El Niño events that have occurred since 1950. Values shown are in units of mm/day, and areas passed 90% significance test using a student-t test are hatched.

sea boards, with the dry anomalies located mostly over the Pacific Northwest and the Great Lakes regions and the wet anomalies located over the Southwest and the Southeast. However, the intensity and the area coverage of the dry and wet anomalies are noticeably different between the two types. The dry anomalies produced by the CP El Niño are of larger magnitudes and cover larger areas than those produced by the EP El Niño. The areas of dry anomalies expand southward to a greater extent during CP El Niños than during EP El Niños. For example, the dry anomalies cover only the Great Lakes region during EP El Niños, but extend southwestward through the Ohio–Mississippi Valley toward the Gulf Coast during CP El Niños. In contrast, the wet anomalies tend to have smaller magnitudes during CP El Niños than during the EP El Niños—a phenomenon that appears most obviously over the Southeast US. Figures 2(a)–(b) indicate that the CP El Niño tends to intensify the dry anomalies but weaken the wet anomalies of the impact pattern produced by the EP El Niño. This important difference is clearly revealed in figure 2(c), where the precipitation anomalies regressed with the EP El Niño were subtracted from the anomalies regressed with the CP El Niño (i.e., figure 2(b) minus figure 2(a)). Figure 2(c) shows negative differences over most of the US, excluding the southern portion of the Southwest where positive differences exist. The negative values in figure 2(c) indicate that a shift in El Niño from the EP type to the CP type makes the dry anomalies over the Pacific Northwest and along the Ohio–Mississippi Valley drier and the wet anomalies over the Southeast less wet. Southern California and Arizona are the only regions where the CP El Niño makes the winter climate wetter than during the EP El Niño events. Overall, the regression analyses reveal that the CP type of El Niño enhances the drying effect of El Niño on US winter precipitation.

To further confirm the different impacts produced by the two types of El Niño, we examined US winter precipitation anomalies during individual EP and CP El Niño years over the following four regions: the Pacific Northwest, Ohio–Mississippi Valley, Southeast and Southwest. Yu *et al* (2012b) have identified twenty-one major El Niño events during 1948–2010 using the Ocean Niño Index and have determined the types of these events based on the consensus of three different identification methods (Kao and Yu 2009, Yeh *et al* 2009, and Ashok *et al* 2007). According to their table 1, eight of the twenty-one El Niño events are of the EP type (1951–52, 1969–70, 1972–73, 1976–77, 1982–83, 1986–87, 1997–98, and 2006–07) while the other thirteen are of the CP type (1953–54, 1957–58, 1958–59, 1963–64, 1965–66, 1968–69, 1977–78, 1987–88, 1991–92, 1994–95, 2002–03, 2004–05, and 2009–10). Figures 2(g)–(i) show the US winter precipitation anomalies composited from these two groups of El Niño events. The dry and wet anomalies produced by these El Niño composites are similar, in general, to the regression results shown in figures 2(a)–(c) that include not only El Niño but also La Niña impacts on US. The composites show dry-north, wet-south patterns for the both types of El Niño, but with the dry anomalies intensified in the CP El Niño composite over the Pacific Northwest and the Ohio–Mississippi Valley and the wet anomalies weakened over the Southeast US.

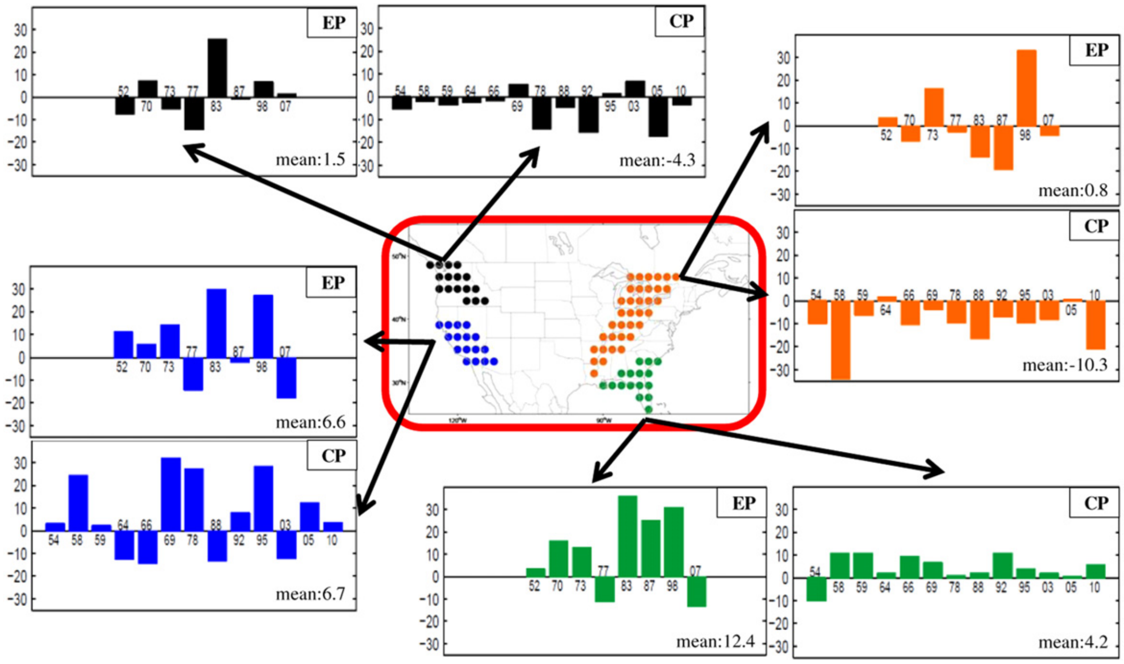

Figure 3. Winter precipitation anomalies averaged separately for the four selected US regions during the 8 major EP El Niño years and the 13 CP El Niño events. The mean anomalies averaged over the EP or CP El Niño events are also shown in the panels in unit of mm/day.

We then examine in figure 3 the winter precipitation anomalies in each of these two groups of El Niño events over the four US regions. The specific grid points used in the averages for each of the regions are indicated in the figure. These points were selected from figure 2 based on the precipitation anomaly centers associated with the both types of El Niño. The stronger drying effect of the CP El Niño over the Pacific Northwest is obvious in figure 3, which shows a mean precipitation anomaly of -4.3 mm d^{-1} for the CP El Niño years but a mean of $+1.5$ mm d^{-1} for the EP El Niño years. Negative anomalies also tend to occur over the Pacific Northwest more consistently during the CP El Niño years (i.e., 10 out of 13 events; 77%) than during the EP El Niño years (i.e., 4 out of 8 events; 50%). This enhanced drying tendency is also very obvious in the Ohio–Mississippi Valley. During eleven of the thirteen CP El Niño years (i.e., 85%), the winter precipitation anomalies over this region are below normal, but the percentage drops to five out of eight (63%) for the EP El Niño years. The mean precipitation anomalies also change from -10.3 mm d^{-1} during the CP El Niño group to $+0.8$ mm d^{-1} for the EP El Niño group. Over the Southeast, both types of El Niño produce wet anomalies; however the precipitation anomalies are very large (with a mean value of $+12.4$ mm d^{-1}) during the EP El Niño winters, but are consistently small during the CP El Niño winters (with a mean value of $+4.2$ mm d^{-1}). This is consistent with the conclusion we draw from figure 2 that the wet anomalies produced by El Niño over the Southeast are weaker during the CP type than during the EP type. Over the Southwest region, positive precipitation anomalies occurred during nine out of the thirteen CP El Niño years (i.e., 69%) and during five out of eight EP El Niño years (62%). The mean precipitation anomalies are $+6.6$ mm d^{-1} for the EP El Niño group and $+6.7$ mm d^{-1} for the CP El Niño group. There are indications of a stronger wetting effect produced by the CP El Niño than the EP El Niño, but the differences are not as significant as those found in the other three regions.

Winter precipitation over the US is primarily associated with winter storms, whose paths across the US are controlled by the locations of tropospheric jet streams. The climatological locations of the jet streams in the winter can be identified by the local maxima in the mean zonal winds at 300 mb ($U_{300\ \mathrm{mb}}$), as shown in figure 4(a). The figure shows that there is a double-jet feature over the West Coast that merges into a single jet over the East Coast (indicated by the black bold lines in the figure). We then separately regressed winter $U_{300\ \mathrm{mb}}$ anomalies onto the EP and CP El Niño indices in figures 4(b) and (c) to examine how the jet streams respond to El Niño. The mean locations of the polar and subtropical jet streams identified from figure 4(a) are superimposed on figures 4(b)–(c) to aid the examination of the jet stream variations. Figures 4(b) and (c) indicate that the jet streams shift southward during both types of El Niño, with large negative wind anomalies in the northern US and large positive wind anomalies in the south. Previous studies have suggested that such an equator-ward shift of the tropospheric jet streams during El Niño events result from El Niño-induced Rossby wave trains and strengthening of the Hadley circulation (e.g., Wang and Fu 2000, Seager *et al* 2003, Lu *et al* 2008). As the jet streams shift southward, winter storms shift south with them, leading to a dry-north, wet-south pattern of precipitation anomalies during the El Niño. However, we find from figure 4 that the jet streams are displaced more southward during CP El Niños than during EP El Niños. Off the West Coast, for example, the weakening of the zonal winds in the north and the strengthening of the

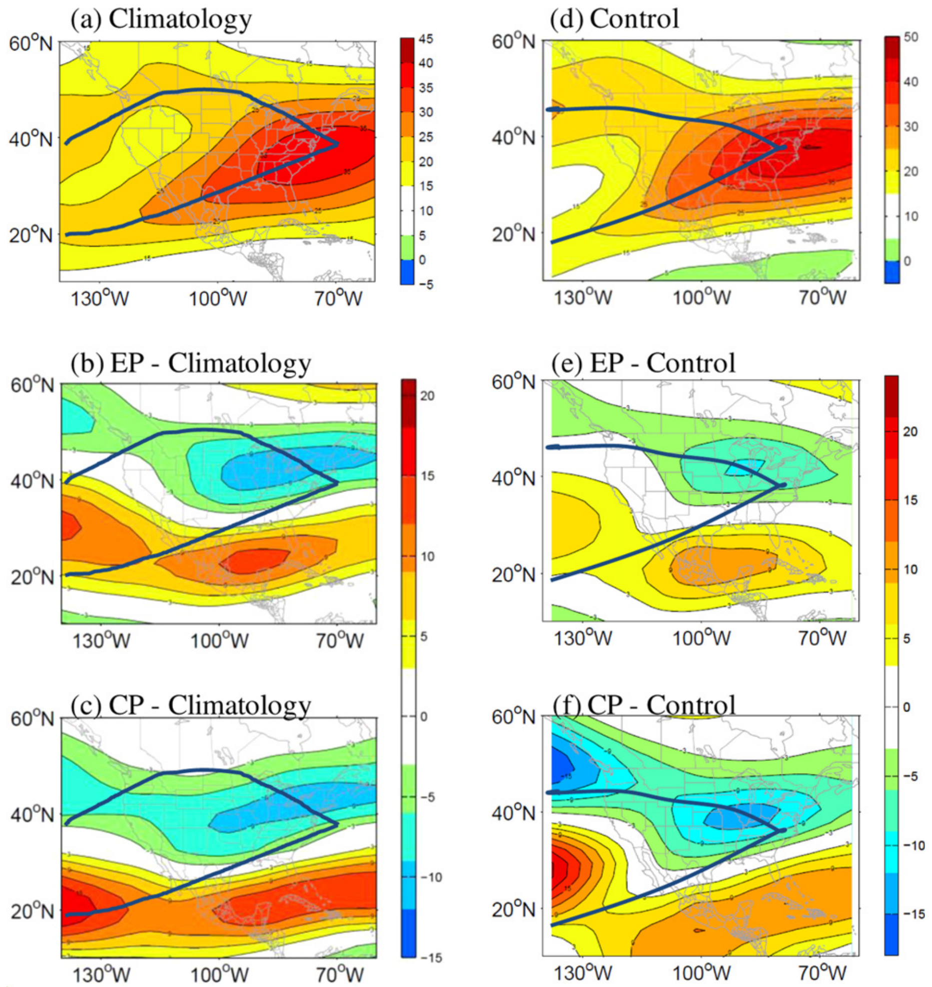

Figure 4. 300 mb zonal winds ($U_{300\ \mathrm{mb}}$) from NCEP/NCAR reanalysis averaged during the winter season (JFM) from 1948 to 2010 (a), and the anomalies regressed to (b) the EP El Niño index and (c) the CP El Niño index. Panels (d)–(f) show, respectively, the ensemble-mean winter $U_{300\ \mathrm{mb}}$ produced by the control run of the forced AGCM experiment, the $U_{300\ \mathrm{mb}}$ differences between the EP El Niño run and the control run, and the differences between the CP El Niño run and the control run. The climatological locations of tropospheric jet streams are indicated by black bold lines along the local maxima of $U_{300\ \mathrm{mb}}$. Units shown are in units of m/s.

winds in the south are centered, respectively, at 55°N and 30°N for the EP El Niño, but at 45°N and 20°N for the CP El Niño. The more southward displacements of the jet streams explain why the dry anomalies over the northern US (including the Northwest and Ohio–Mississippi Valley) expand and strengthen more significantly during CP El Niños than during EP El Niños. Similarly, the wet anomalies over the southern US expand over the Southwest and extend into the Mexico during the CP El Niño. However, the same southward displacements over the East Coast push the core of the subtropical jet stream (and therefore the storm tracks) out of the US continent and into the Gulf and Caribbean, which results in only a small area of wet anomalies left in the Southeast US during the CP El Niño.

To further verify the different impacts of the two types of El Niño, we contrast in figures 2(d)–(f) the US winter precipitation anomalies calculated from the three forced AGCM ensemble experiments. The impacts produced by the EP and CP types of El Niño on the US winter precipitation were identified by subtracting the ensemble mean of the control run from the ensemble means of the EP and CP runs. It is encouraging to find that the CAM4 experiments reproduce the major findings obtained from the regression analyses (cf figures 2(a)–(c)): the CP El Niño enhances the dry impacts and weakens the wet impacts on US winter, except over the Southwest. Compared to the EP run, the CP run produces stronger dry anomalies over the US Northwest and Ohio–Mississippi Valley and weaker wet anomalies over the Southeast. It is particularly interesting to note that the CP run reproduces the strong dry anomalies along the Ohio–Mississippi Valley previously revealed in the analysis of NCEP–NCAR reanalysis (cf figures 2(e) and (b)). The tendency toward wetter anomalies over the Southwest during the CP El Niño is more evident in the forced CAM4 experiments than in the regression results. We also examined the 300 mb zonal wind ($U_{300\ \mathrm{mb}}$) anomalies from the forced AGCM experiments (shown in figures 4(e)–(f)) and noted that similar southward shift of the jet streams during the two types of El Niño can be seen in these model results. Particularly, the jet streams in the CP El Niño run displace more southward over the eastern half of the US than in the EP El Niño run, which is consistent with the result obtained from the regression analysis with the reanalysis product. It should be noted that the $U_{300\ \mathrm{mb}}$ climatology produced by the CAM4 model over the US is reasonably realistic (figure 4(d)).

4. Conclusions

We performed analyses with reanalysis products and numerical experiments to show that the recently emerged CP type of El Niño can enhance the dry impacts and weaken the wet impacts produced by the traditional EP type of El Niño on US winter precipitations. While both types of El Niño shift the jet streams southward from their climatological winter locations over the US, the shift is larger during the CP El Niño. Since the paths that winter storm moves over the US continent are steered by the jet streams, the more southward shift of the jet streams explains why the dry anomalies that El Niño typically produced over the Pacific Northwest and Ohio–Mississippi Valley expand their covering areas and increase their intensities during the CP El Niño. The more southward shifts of the jet streams are supposed to increase the storm activities and the winter precipitations over the Southwest and Southeast. However, the core of the jet streams along the eastern US moves to the Gulf during the CP El Niño and reduces the land area of wet anomalies over the US Southeast. The southern end of the Southwest is the only region of the US that is exempted from the drying effect produced by El Niño when it shifts from the EP type to the CP type.

One major implication from this study is that droughts occurred in the Ohio–Mississippi Valley and Pacific Northwest during El Niño years may be intensified after the El Niño becomes more of the CP types, and the Southeast cannot expect as much supply of winter precipitations during El Niño years as in the past. At the same time, the Southwest should prepare for more severe flooding events during CP El Niño years. Another major implication from this study is that the shift of the El Niño from the EP type to the CP El Niño in recent decades may have produced a net drying effect on the US winter precipitations, except over the Southwest. Since the CP El Niño is known to have occurred more frequently in the recent decades, particularly after the 1990, its possible linkage with the extended US drought since the 1990s deserves further investigations.

Acknowledgments

We thank the anonymous reviewers for their valuable comments. This research was supported by NOAA-MAPP Grant NA11OAR4310102 and NSF Grant ATM-1233542.

References

Ashok K, Behera S K, Rao S A, Weng H and Yamagata T 2007 El Niño Modoki and its possible teleconnection *J. Geophys. Res.* **112** C11007
Barsugli J J and Sardeshmukh P D 2002 Global atmospheric sensitivity to tropical SST anomalies throughout the Indo-Pacific basin *J. Clim.* **15** 3427–42
Cayan D R, Redmond K T and Riddle L G 1999 ENSO and hydrologic extremes in the western United States *J. Clim.* **12** 2881–93
Dettinger M D, Cayan D R, Diaz H F and Meko D M 1998 North–south precipitation patterns in western North America on interannual-to-decadal timescales *J. Clim.* **11** 3095–111
DeWeaver E and Nigam S 2004 On the forcing of ENSO teleconnections by anomalous heating and cooling *J. Clim.* **17** 3225–35
Guan B and Nigam S 2008 Pacific sea surface temperatures in the twentieth century: an evolution-centric analysis of variability and trend *J. Clim.* **21** 2790–809
Hoerling M P and Kumar A 2002 Atmospheric response patterns associated with tropical forcing *J. Clim.* **15** 2184–203
Kao H-Y and Yu J-Y 2009 Contrasting Eastern-Pacific and Central-Pacific types of ENSO *J. Clim.* **22** 615–32
Kiladis G N and Diaz H F 1989 Global climatic anomalies associated with extremes in the southern oscillation *J. Clim.* **2** 1069–90
Kistler R *et al* 2001 The NCEP–NCAR 50–Year Reanalysis: monthly means CD–ROM and documentation *Bull. Am. Meteorol. Soc.* **82** 247–67
Kug J-S, Jin F-F and An S-I 2009 Two types of El Niño events: cold tongue El Niño and warm pool El Niño *J. Clim.* **22** 1499–515
Kumar A and Hoerling M P 1995 Prospects and limitations of seasonal atmospheric GCM predictions *Bull. Am. Meteorl. Soc.* **76** 335–45
Larkin N K and Harrison D E 2005a Global seasonal temperature and precipitation anomalies during El Niño autumn and winter *Geophys. Res. Lett.* **32** L16705
Larkin N K and Harrison D E 2005b On the definition of El Niño and associated seasonal average US weather anomalies *Geophys. Res. Lett.* **32** L13705
Lee T and McPhaden M J 2010 Increasing intensity of El Niño in the central-equatorial Pacific *Geophys. Res. Lett.* **37** L14603
Livezey R E, Masutani M, Leetmaa A, Rui H, Ji M and Kumar A 1997 Teleconnective response of the Pacific-North American region atmosphere to large central equatorial Pacific SST anomalies *J. Clim.* **10** 1787–820
Lu J, Chen G and Frierson D M W 2008 Response of the zonal mean atmospheric circulelation to El Niño versus global warming *J. Clim.* **21** 5835–51
Mo K C 2010 Interdecadal modulation of the impact of ENSO on precipitation and temperature over the United States *J. Clim.* **23** 3639–56
Mo K C and Higgins R W 1998 The Pacific–South American modes and tropical convection during the Southern Hemisphere winter *Mon. Weather Rev.* **126** 1581–96
Mo K C and Higgins R W 1998 Tropical convection and precipitation regimes in the western United States *J. Clim.* **11** 2404–23
Montroy D L, Richman M B and Lamb P J 1998 Observed nonlinearities of monthly teleconnections between tropical Pacific sea surface temperature anomalies and central and eastern North American precipitation *J. Clim.* **11** 1812–35
Ropelewski C F and Halpert M S 1986 North America precipitaion and temperature associated with the El Niño/Southern Oscillation (ENSO) *Mon. Weather Rev.* **114** 2352–62
Ropelewski C F and Halpert M S 1989 Precipitation patterns associated with the high index phase of the Southern Oscillation *J. Clim.* **2** 268–84
Seager R, Harnik N, Kushnir Y, Robinson W and Miller J 2003 Mechanisms of hemispherically symmetric climate variability *J. Clim.* **16** 2960–78

Smith T M and Reynolds R W 2003 Extended reconstruction of global sea surface temperatures based on COADS data (1854–1997) *J. Clim.* **16** 1495–510

Trenberth K E and Stepaniak D P 2001 Indices of El Niño evolution *J. Clim.* **14** 1697–701

Wallace J M and Gutzler D S 1981 Teleconnections in the geopotential height field during the Northern Hemisphere winter *Mon. Weather Rev.* **109** 784–812

Wang C and Weisberg R H 2000 The 1997–98 El Niño evolution relative to previous El Niño events *J. Clim.* **13** 488–501

Wang H and Fu R 2000 Influences of ENSO SST anomalies and winter storm tracks on the interannual variability of upper-troposphere water vapor over the Northern Hemisphere Extratropics *J. Clim.* **13** 59–73

Yeh S -W, Kug J -S, Dewitte B, Kwon M -H, Kirtman B P and Jin F -F 2009 El Niño in a changing climate *Nature* **461** 511–4

Yu J -Y and Kao H -Y 2007 Decadal changes of ENSO persistence barrier in SST and ocean heat content indices: 1958–2001 *J. Geophys. Res.* **112** D13106

Yu J -Y and Kim S T 2010 Three evolution patterns of Central-Pacific El Niño *Geophys. Res. Lett.* **37** L08706

Yu J -Y, Lu M -M and Kim S T 2012a A change in the relationship between tropical central Pacific SST variability and the extratropical atmosphere around 1990 *Environ. Res. Lett.* **7** 034025

Yu J -Y, Zou Y, Kim S T and Lee T 2012b The changing impact of El Niño on US winter temperatures *Geophys. Res. Lett.* **39** L15702